Characterization of Anisotropic Behaviour of ZK60 Extrusion under Stress-control Condition and Notes on Fatigue Modeling

A.H. Pahlevanpour, S.B. Behravesh, S. Adibnazari, H. Jahed

PII: S0142-1123(19)30204-X
DOI: https://doi.org/10.1016/j.ijfatigue.2019.05.030
Reference: JIJF 5133

To appear in: *International Journal of Fatigue*

Received Date: 5 November 2018
Revised Date: 20 May 2019
Accepted Date: 25 May 2019

Please cite this article as: Pahlevanpour, A.H., Behravesh, S.B., Adibnazari, S., Jahed, H., Characterization of Anisotropic Behaviour of ZK60 Extrusion under Stress-control Condition and Notes on Fatigue Modeling, *International Journal of Fatigue* (2019), doi: https://doi.org/10.1016/j.ijfatigue.2019.05.030

Characterization of Anisotropic Behaviour of ZK60 Extrusion under Stress-control Condition and Notes on Fatigue Modeling

A.H. Pahlevanpour[1-2], S.B. Behravesh[1], S. Adibnazari[2], H. Jahed[1*]

[1]Deparment of Mechanical & Mechatronics Engineering, University of Waterloo, 200 University Ave W, Waterloo, ON N2L 3G1, Canada

[2]Department of Aerospace Engineering, Sharif University of Technology, Azadi Street, Tehran, Iran

Abstract

The anisotropic fatigue behavior of ZK60 is investigated through stress-control tests along two different material directions: extrusion (ED) and radial (RD) directions. The in-plane random texture along RD promotes activation of twinning/detwinning deformations in both tension and compression reversals, which brings about a sigmoidal but near-symmetric shape for hysteresis loops. The stress-strain response along ED is asymmetric, which is attributed to different deformation mechanisms in tension and compression reversals. The higher fatigue strength along ED is related to lower plastic strain energy in this direction. An energy damage parameter showed a good correlation with tests performed in RD and ED.

Keywords: Wrought Magnesium, Characterization, Fatigue Modeling, Anisotropy, Stress-control

Introduction

Environmental concerns, as well as economical considerations, have shaped car manufacturers' strategies toward cutting fuel consumption in vehicles. Reducing weight by adopting lightweight materials, such as magnesium (Mg) alloys, has been a key approach to achieving this goal [1]. In spite of the very low density (1.8 g/cm^3) that makes Mg the lightest structural metal, its applications have been limited. One challenge of applying Mg alloys in load-bearing components is their complex mechanical behavior, which arises from their hexagonal close-packed (HCP) crystallographic structure. This complexity is more pronounced in textured wrought alloys than in cast alloys [2]. Asymmetry (dissimilar

* Corresponding author, hamid.jahed@uwaterloo.ca

behavior under tension and compression) and anisotropy (dissimilar behavior in different material orientations) are two main mechanical characteristics of wrought Mg alloys. Activation of $\{10\bar{1}2\}$ extension-twinning deformation mechanism, when the external load provokes extension along the c-axis in HCP crystals in one direction and slip-dominant deformation in the reverse direction, introduces distortion into loading-unloading curve. This behavior is known as asymmetry [3], which is different from strength-differential effect happening in high-strength cubic materials [4]. Forming processes such as rolling or extrusion render the c-axis perpendicular to the forming direction, bringing about an intensive basal texture, and eventually causing anisotropy in wrought Mg alloys [2].

Asymmetry and anisotropy have been extensively reported and discussed in the literature on wrought Mg alloys under cyclic loading. Numerous studies have presented such a behavior under strain-control fatigue tests, covering a wide range of wrought Mg alloys, including AM30 [5], [6], AM50 [7], AZ31 [8]–[13], AZ61 [14], AZ80 [15], AZ91 [16], ZA81 [17], and ZK60 [18]–[20]. However, fewer studies have inquired into the anisotropy and asymmetry in the stress-controlled fatigue behavior of wrought Mg alloys [7], [9], [12], [16], [21]–[24]. Park et al. [12] reported that redirecting loading from rolling direction to normal to the rolled plane (ND), reduces the fatigue strength of wrought AZ31 significantly. This behavior has been attributed to the greater degree of plastic-strain-induced damage in ND, arising from the reduced twinning stress of ND specimens under tension. Zhang et al. [23] conclusively showed that the cyclic softening-to-hardening transition observed in hot-rolled AZ31B is insensitive to both specimen orientation and rolling percent-reduction. The anisotropic fatigue behavior of ZK60 extrusion under stress-controlled condition has not been addressed explicitly.

Stress, strain, and energy are three common approaches to modeling the fatigue behavior of Mg alloys. The fully reversed stress-control behavior has been appropriately expressed using a stress-based fatigue model proposed by Basquin [25]. Later, the Coffin-Manson strain-based relation quantified the strain-life curve in low-cycle (LCF) and high-cycle fatigue (HCF) regimes [26]. Feltner & Morrow were the first to suggest strain energy density as a fatigue damage parameter [27]. Plastic strain energy density (PSED)

accumulated in the stabilized stress-strain hysteresis loops was used by Garud [28] and Lefebvre et al. [29] as an energy-based damage criterion. Ellyin [30], [31] combined PSED with elastic strain energy density (ESED), suggesting the concept of total strain energy density (TSED) to take into account the mean stress effect. The above-mentioned approaches have been adopted to predict the fatigue life of wrought Mg alloys under stress-controlled conditions [16], [24], [32]–[35].

A study by Ishihara et al. [36] on AZ31 extrusion under different cyclic load ratios demonstrated that the Greber model's performance was superior to that of the modified Goodman model in predicting the fatigue life of stress-controlled experiments. Hasegawa et al. [35] added a correction term to the Coffin-Manson equation in order to improve its accuracy for the life prediction of AZ31 extrusion. The new model provided reliable predictions under stress-control condition, while the life was over-estimated for the strain-controlled tests, exhibiting retained asymmetry in the stress-strain response of the material. The inability of the Smith [37], Smith–Watson–Topper [38], and Paul–Sivaprasad–Dhar [39] models to predict the fatigue life of rolled AZ91 in rolling and transverse directions led to the proposal of a modified Basquin's equation [16]. It accounted for the mean stress effect by introducing a new definition for the fatigue strength coefficient (σ'_f) and fatigue strength exponent (b). Shiozawa et al. [32] applied different models to predicted the fatigue life of AZ31, AZ61, and AZ80 extrusion alloys under both strain- and stress-controlled experiments. They found that TSED, as a fatigue damage parameter, was superior to the plastic strain range and PSED. Park et al. [34] showed that Ellyin's criterion provides reliable predictions for different strain and stress ratios. Chen et al. [40] revised the conventional definition of ESED in the Ellyin's model in an attempt to enhance the life prediction accuracy for AZ31B extrusion in a corrosive environment with mean stress. For this purpose, they incorporated both the positive and negative elastic energy densities into the ESED. Dallmeier et al. [7] weighted the elastic portion of strain energy to capture the mean stress sensitivity of strain-life and stress-life curves for twin roll cast AM50 in two directions. They identified compressive yield stress (CYS) as a reference limit, beyond which twinning was significantly activated, followed by distinct hardening and pronounced increase in the area

surrounded by stress-strain hysteresis loops, representing PSED.

Among the different approaches applicable to explain the fatigue behavior of wrought Mg alloys, the energy approach possesses great potentials to describe the damage in different material orientations using a scalar quantity as a damage parameter, i.e., the strain energy density. Energy-based models are commonly differentiated by the definition of ESED and the mathematical expression that correlates the damage parameter to the fatigue life [31]. Jahed and Varvani [41] introduced a fatigue model (JV) based on the governing crack nucleation and propagation mechanisms, along with the plastic energy accumulated by cyclic deformation. In order to extend the original model's applicability to handle non-proportional loading, the incremental cyclic plasticity of Garud was embedded into the strain energy calculation [42]. The JV model has been successfully employed for the fatigue life correlation of Mg alloys in several studies [43]–[45]. Roostaei et al. [5] and Pahlevanpour et al. [20] demonstrated the auspicious capability of the JV damage parameter in the anisotropic fatigue life prediction of AM30 and ZK60 extrusion, respectively under strain-control condition. The predictions were made with a single set of material parameters extracted in one specific direction to assess the model's insensitivity to the loading direction. The ability of energy-based models to explain the fatigue damage of metals under different loading conditions, i.e., stress- and strain-control, and along various material's directions using a single set of parameters has yet to be examined.

This study characterizes the fatigue behavior of ZK60 extrusion under stress-controlled condition in two perpendicular directions: the extrusion direction (ED) and radial direction (RD). Special attention is given to a detailed explanation of the observed anisotropy and asymmetry. The effect of initial texture on strain and stress-strain hysteresis evolutions under stress control cyclic tests is discussed. Different mechanisms in strain accumulation under constant amplitude stress controlled tests is studied. Some modeling considerations regarding the suitability of an energy damage parameter is presented. The results demonstrate promising correlations between the experimental and predicted fatigue lives in different material orientations for both the stress- and strain-controlled loading conditions.

1.1. Material and Specimens

A cylindrical billet with a diameter of 127 mm made of commercial ZK60 extrusion and supplied by Magnesium Elektron of North America (MENA) was used in the current study. The raw material is identical to the one previously investigated in another study by the authors [20]. The chemical composition of the studied ZK60 extrusion is set out in Table 1. The dog-bone specimens, with the geometry depicted in Figure 1 (a) were machined along RD and ED according to the cylindrical coordinate system, as illustrated in Figure 1 (b). In this figure, TD denotes the tangential direction.

Table 1. Chemical composition of ZK60 extrusion

Element	Zn	Zr	other	Mg
wt.%	5.5	0.71	<0.3	balanced

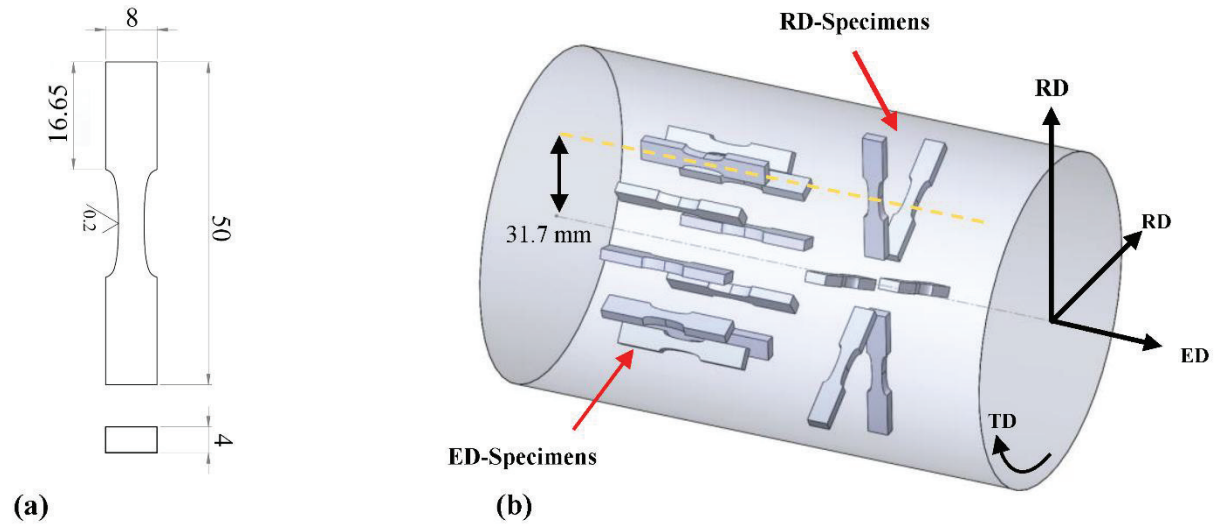

Figure 1. a) Dog-bone specimens' geometry (units in mm) and b) Specimens' orientations machined from ZK60 extrusion billet

1.2. Experimental procedures

All tests were conducted at the room temperature, using a servo-hydraulic Instron 8874 test frame. Fully reversed (R=-1) stress amplitudes were imposed in the range of 70 to 200 MPa at a cyclic frequency of up to 10 Hz. In general, loading cycle was initiated by a tensile reversal and followed by a sinusoidal waveform. Engineering strain was measured throughout the tests using an Instron extensometer with a gauge length of 10 mm and a ±1 mm travel. For each stress amplitude, at least two specimens were tested

to ensure reproducibility of test results, and N_f denotes the number of cycles corresponding to final fracture. Tests were interrupted after 10^6 cycles, and the life was considered infinite.

2. Experimental Results and Discussion

Texture analyses in the literature have demonstrated that the extrusion process on ZK60 renders the c-axes perpendicular to the ED but randomly distributes them in the RD-TD plane [18], [20], [46]. Figure 2 and Table 2 summarize the quasi-static tests results along ED and RD that the authors obtained in an earlier study [20]. The large difference in the tensile and compression yield strengths of specimens loaded along ED revealed intense asymmetry, which is attributed to easily activated extension twins along ED under compression [20], [47]. In contrast, the undirected dispersion of the HCP crystals in the RD-TD plane provides an equal chance of extension twinning in both tension and compression for RD specimens, resulting in almost symmetrical behavior [20].

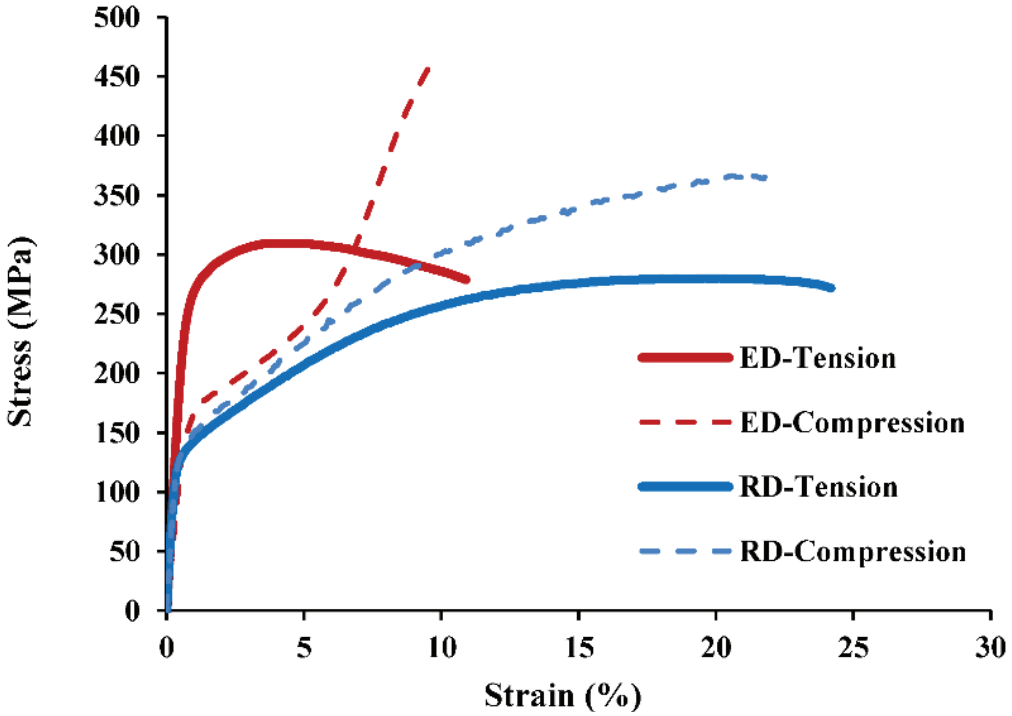

Figure 2. Quasi-static stress-strain curves for ZK60 extrusion under uniaxial tension and compression [20]

Table 2. Average mechanical properties of ZK60 extrusion along ED and RD (The numbers inside the parentheses denote standard deviation) [20]

Mechanical properties	ED	RD
Modulus of elasticity [GPa]	43 (1)	45 (0)
Tensile yield strength [MPa]	251 (0)	128 (0)
Tensile ultimate strength [MPa]	309 (1)	279 (1)
Compressive yield strength [MPa]	128 (10)	132 (4)
Compressive ultimate strength [MPa]	449 (15)	357 (9)

2.1. Fatigue behavior

2.1.1. Radial Direction

Figure 3 illustrates the evolution of strain in the first loading cycle for an RD specimen loaded to the stress amplitude of $\sigma_a = 200$ MPa. In the first tensile reversal, beyond the tensile yield strength (TYS), basal slip dominates the plastic deformation at low stress levels. However, due to the undirected crystallographic orientation in the RD-TD plane, $\{10\bar{1}2\}$ pyramidal twinning may be triggered at high stress levels [20]. The first tensile reversal plastically deforms the specimen up to 4% of strain by simultaneous activation of slip and extension twinning, with slip being the dominant mechanism, contributing to low TYS. In the subsequent reversal, detwinning of formerly twinned grains in conjunction with the twinning of untwinned grains predominantly strain the specimen. At the end of the unloading stroke, 1.7% compressive strain will be imposed which is lower compared to 4% tensile strain achieved at the end of loading. Reloading the sample in tension deforms it by means of the detwinning followed by non-basal slip up to 3.5 %, instead of the prior 4 % strain experienced in the initial loading. This difference generates a 0.5% strain gap within the unclosed hysteresis loop, in the form of the mean strain, as indicated in Figure 3. This directional and escalating mean strain is referred to as “cyclic strain ratcheting” [48]. In metals with symmetric tension-compression curves, ratcheting takes place by virtue of mean stress [49], whereas in wrought Mg alloys fully reversed loading with no mean stress will induce a substantial amount of ratcheting due to asymmetric cyclic hardening behavior. The mutual participation of twinning and slip in both tensile and compressive reversals yields sigmoidal but the near-symmetric shape of the hysteresis loop for the first cycle along RD.

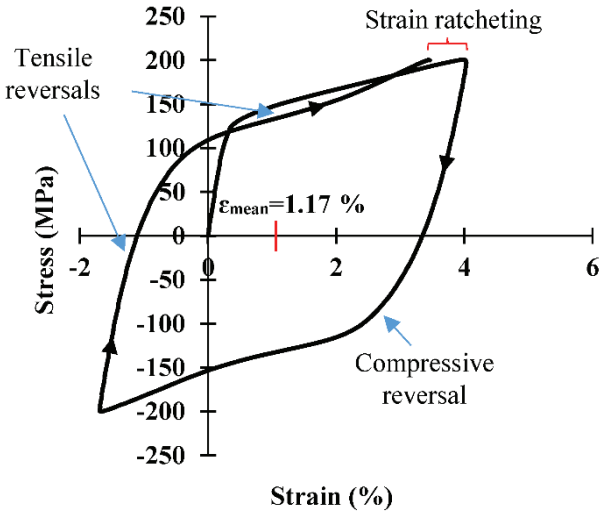

Figure 3. Strain ratcheting in the first cycle along RD at σ_a = 200 MPa

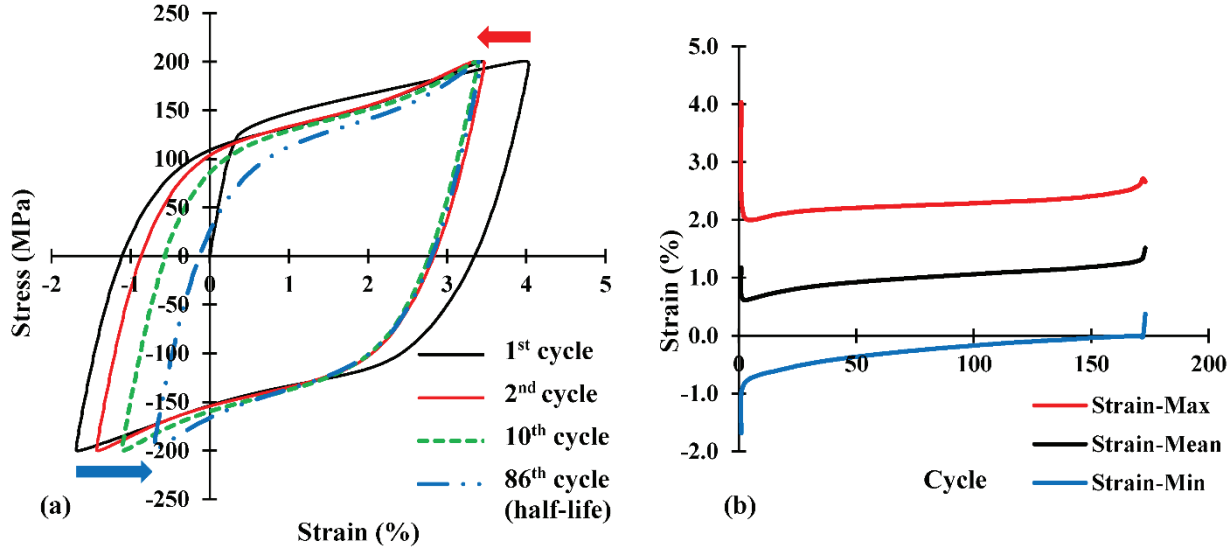

Figure 4. a) Evolution of stress-strain hysteresis loops along RD at σ_a = 200 MPa and b) Strain evolution along RD at σ_a = 200 MPa

Figure 4 (a) shows the progressive strain ratcheting through stress-strain fatigue hysteresis loops. The near-symmetric shape of the first cycle's stress-strain response is sustained during cyclic loading; however, the size of the hysteresis loop shrinks significantly. The translation of the maximum and minimum strain in opposite directions, as depicted in Figure 4 (a), governs the observed reduction in the size of the hysteresis loops. It is interesting to note that the maximum strain development is almost saturated after the first cycle; however, the minimum strain continues to decline (Figure 4 (b)). This

contrasting behavior can be attributed to deficient detwinning and residual twins impeding the plastic deformation during tensile reversals [50]. The analogous characteristics were perceived for lower stress amplitudes, e.g. $\sigma_a = 140$ MPa, by comparing the first and half-life hysteresis loops of the RD specimens illustrated in Figure 5 (a) and (b), respectively. The only dissimilarity is the concave shape of the hysteresis loops at low stress amplitudes, which can be ascribed to the disabled twinning-detwinning due to insufficient stress.

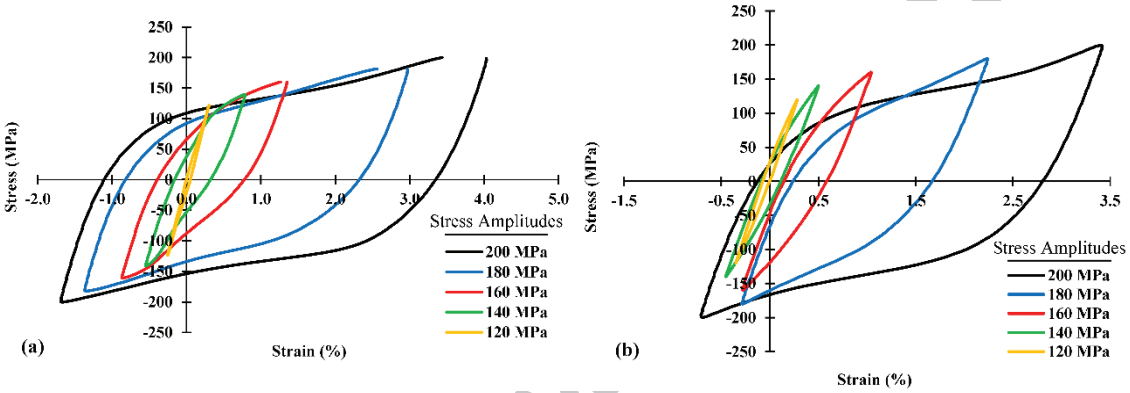

Figure 5. Stress-strain hysteresis loops along RD at different stress amplitudes, ranging from σ_a = 120 to 200 MPa: (a) for the 1st cycle and (b) for the half-life cycle

2.1.2. Extrusion Direction

Figure 6 shows the stress-strain hysteresis response in the first loading cycle along ED for $\sigma_a = 200$ MPa. The high TYS in ED, i.e. 238 MPa, compared to 200 MPa maximum stress, places the first reversal in the elastic region. By reversing the load, the basal texture favors extension twinning activation, resulting in 86.3° rotation of the crystallographic lattice with respect to the loading direction [19]. Twinning in compression reduces CYS against TYS [51], typically referred to as asymmetry, and brings about a significant amount of strain (-4.5 %) at the end of the unloading reversal. The twinned lattices are favorably aligned to detwin during the subsequent tensile loading. Detwinning reorients the twinned grains; however, complete texture restoration is unattainable, and residual twins develop [3]. Detwinning exhausts before reaching the maximum tension where harder non-basal slip takes over and accommodates deformation at yet a higher strain-hardening rate [19], [52]. This substitution turns the concave-down loading curve into a sigmoidal one due to the higher stress demands of non-basal slip mechanisms. The

discussed asymmetric behavior of the material leaves a gap in the hysteresis loop, as illustrated in Figure 6 and results in accumulating ratcheting strain.

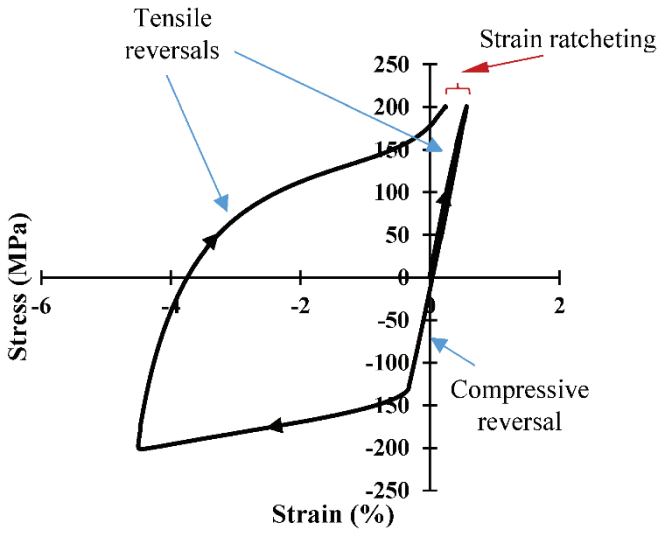

Figure 6. Strain ratcheting in the first cycle along ED at σ_a=200 MPa

Figure 7 (a) depicts the cyclic ratcheting of an ED specimen subjected to $\sigma_a = 200$ MPa. The smooth transition from an asymmetric hysteresis response in the first cycle to a fully symmetric hysteresis in the half-life cycle (cycle #475) can be perceived. This characteristic suggests that twinning and detwinning are the dominant deformation mechanisms in first few cycles, but are replaced by dislocation slip in subsequent cycles. The continuous but decaying evolution of maximum and minimum strains in ED, as shown in Figure 7 (b), shrinks the hysteresis loops, analogous to the behavior observed in RD. Significant irreversible deformation in the first few cycles and the residual twins development that obstruct later plastic deformation prevent the twinning-detwinning from governing plastic deformation with increasing loading cycles and induce a pronounced hardening, reflected in the strain range reduction [51]. Figure 8 illustrates the hysteresis loops corresponding to the first and half-life cycles in different stress amplitudes. By comparing Figure 8 (a) and (b) and tracking the alternation of stress-strain responses at each stress amplitude, a transition from asymmetric to symmetric hysteresis is notable for $\sigma_a > 150$ MPa. However, at lower stress levels, the twinning-detwinning cannot be triggered even in the initial cycles, which puts the slip in charge for the entire history of plastic deformation.

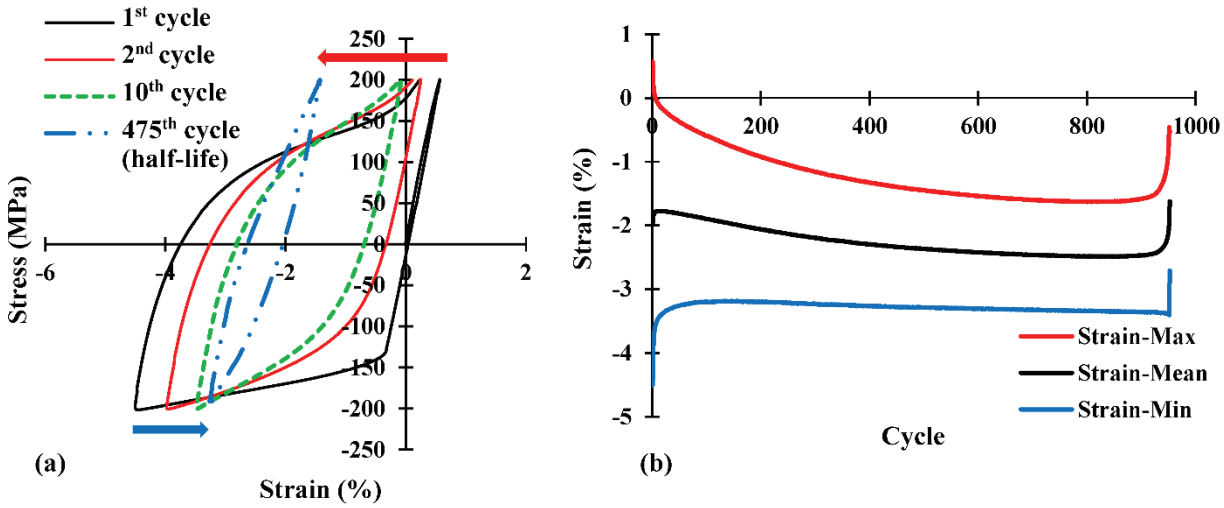

Figure 7. a) Evolution of stress-strain hysteresis loops along ED at σ_a = 200 MPa and b) Strain evolution along ED at σ_a = 200 MPa

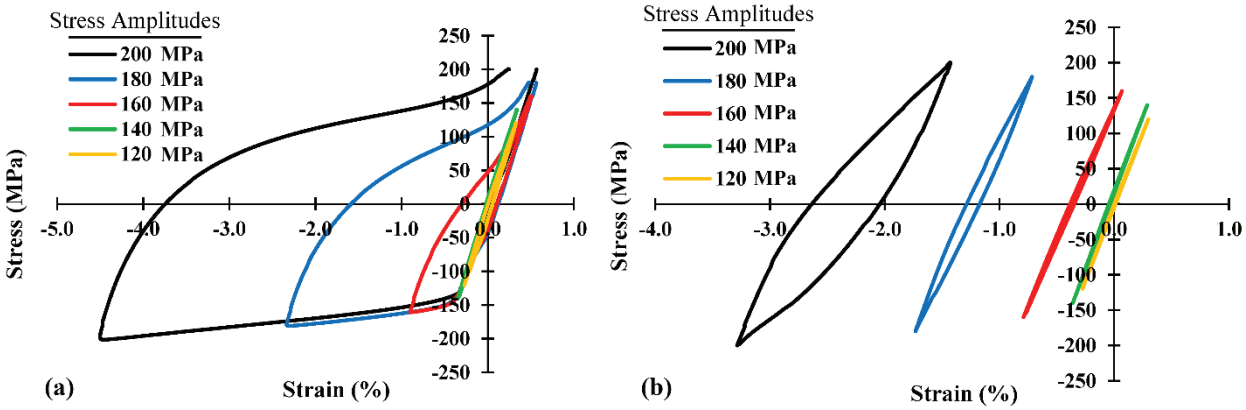

Figure 8. Stress-strain hysteresis loops along ED at different stress amplitudes, ranging from σ_a = 120 to 200 MPa: (a) for the 1st cycle and (b) for the half-life cycle

2.2. Stress-life curve

Figure 9 displays the stress-life curve for ZK60 extrusion along ED and RD. Data-points with arrows indicate run-out tests at 10^6 cycles. The selection of 10^6 cycles for infinite life is corroborated by the literature, which reports the minimal slope of stress- and strain-life curves for Mg alloys in the range of $10^6 < N_f < 10^8$ cycles [7], [53]. The anisotropic quasi-static behavior of ZK60 extrusion is extended to its cyclic behavior as well. The material along ED exhibits superior fatigue performance compared to RD at all stress levels. This behavior contrasts with observed identical LCF strain-controlled behavior in ED and RD [20]. As exemplified in Figure 10, ED specimens show smaller hysteresis loops and consequently less

plastic-induced damage at the same load level compared to RD, which can justify the superior fatigue strength of ED specimens. The gap perceived in the number of cycles to failure for the two loading directions is sustained through all stress levels.

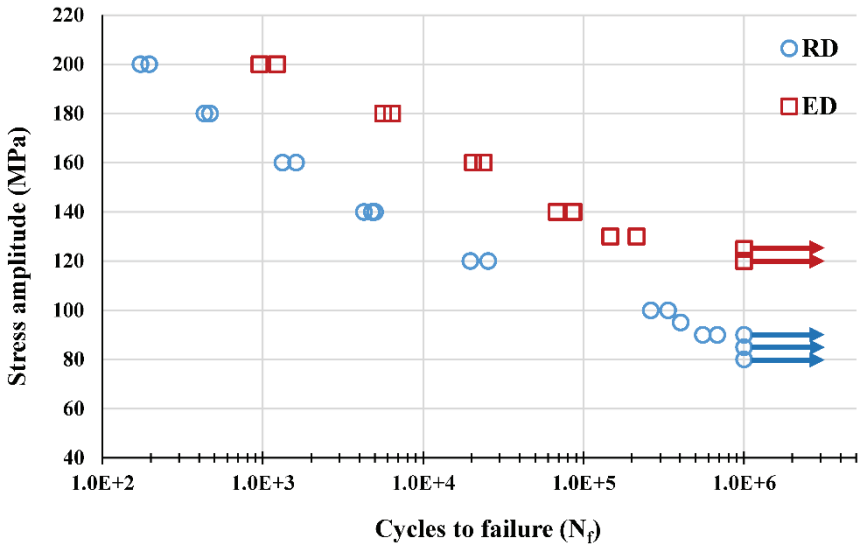

Figure 9. Stress-life curves for RD and ED

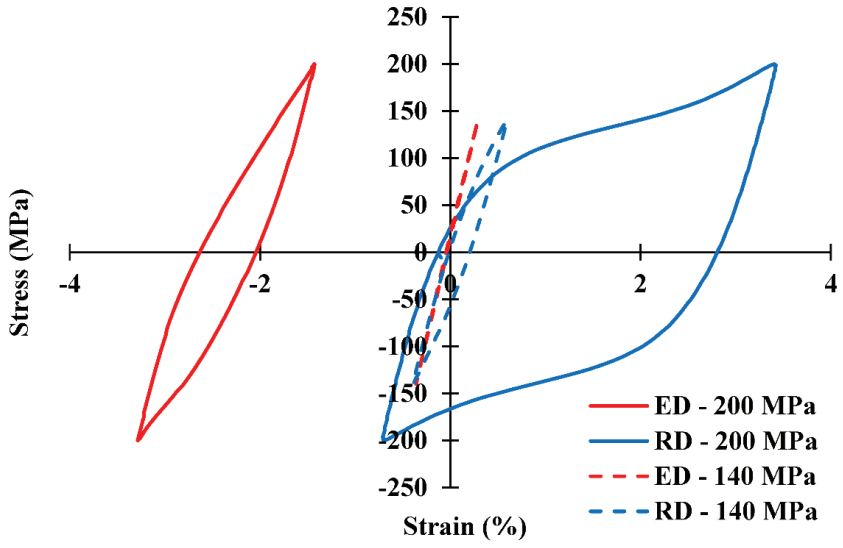

Figure 10. Smaller half-life hysteresis loops of ED compared to RD in two stress amplitudes

Fatigue strength in each direction was quantified by sequentially testing a set of specimens in accordance with the staircase statistical analysis method described in ISO-12107 [54]. The fatigue strength at 10^6 cycles was found equal to 87 MPa and 120 MPa for RD and ED specimens, respectively.

2.3. Initial loading and ratcheting strain effects on fatigue life

The Effect of mean stress on the fatigue strength of Mg alloys has been a major area of interest for researchers [55]–[60]. However, the literature suggests that in the absence of mean stress, the mean strain itself does not significantly affect the life [7], [34], [61]. In order to examine the potential effect of mean strain on fatigue of ZK60 extrusion and also to examine the initial loading effect, cyclic loading was applied with $\sigma_a = 200$ MPa along both RD and ED, with the first reversal being compressive, unlike in the previous experiments, where the first reversal was tensile. When the RD specimens are initially loaded in compression (Figure 11), a negative mean strain compared to the positive one in the tension-first experiments (Figure 3), is induced. The inceptive compressive strain is compensated for by postive strain ratcheting in the subsequent cycles, even though, the half-life mean strain ends up samller than that with tension-first loading. Therfore, as depicted in Figure 12, the dissimilar initial stroke results in a mismatched half-life mean strain for RD; however, the cycles to failure remain close due to the analogous hysteresis-loop shapes. In contrast to RD, the half-life hysteresis along ED for both the loading sequences are almost identical. The similarity can be described by the fully elastic behavior along ED in the first tensile reversal, i.e., the first reversal induced almost no residual strain at zero stress point of the unloading/compressive reversal (Figure 6). Therefore, the material experiences the same plastic deformation history for the two loading sequences, resulting in an identical half-life response.

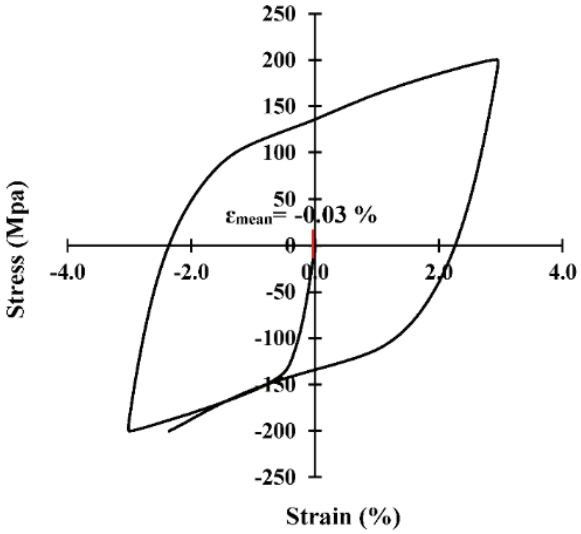

Figure 11. Initial mean strain for the compression first test under 200 MPa stress amplitude

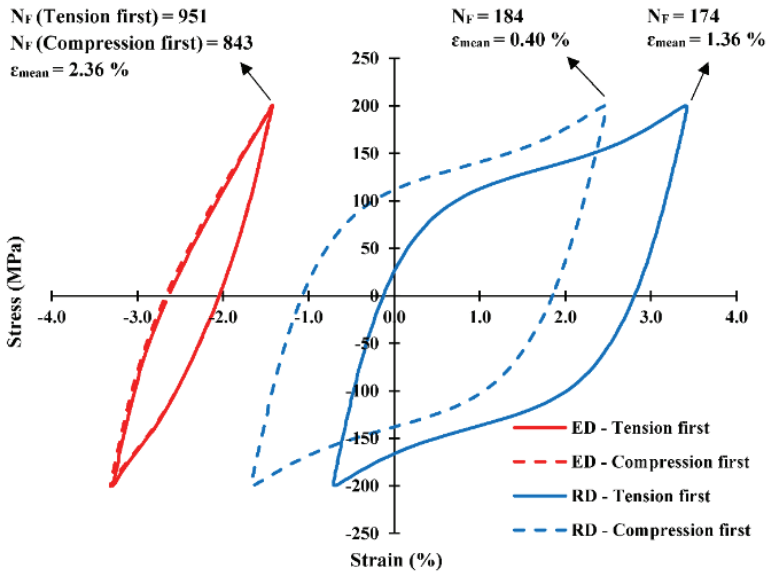

Figure 12. Effect of loading sequence on half-life hysteresis loops for ZK60 extrusion under σ_a = 200 MPa

3. Fatigue Modeling

3.1. Stress-Based Model

The strain response of ZK60 under stress-controlled condition are substantially different along RD and ED, as displayed in Figure 5 and Figure 8. The different cyclic hysteresis behavior of the material in these two directions demonstrates that under the same loading condition, i.e., the same stress amplitude in RD and ED, the damage induced in each loading cycle in one direction is different than that in the other direction. Therefore, one can expect that stress amplitude, as the damage parameter, will not be successful to explain the fatigue damage and to predict the life along these two material directions.

In order to mathematically express the stress-life curves along two directions via a stress-based model, the classical Basquin equation was employed [48]:

$$\sigma_a = A(N_f)^B \qquad \text{Eq. 1}$$

where σ_a is the imposed stress amplitude, and A and B are material constants. Figure 13 depicts the stress-life curve for ZK60 extrusion along RD and ED, indicating the A and B constants for the two directions. Because the A and B parameters are dissimilar along different directions, using one set of

material's parameters will not be successful for the life prediction.

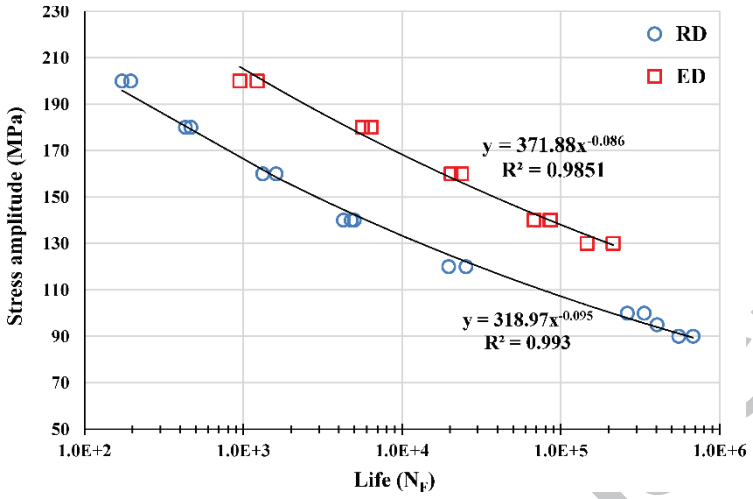

Figure 13. Basquin equation fitted to the stress-life curves of RD and ED

In order to facilitate fatigue modeling, it would be ideal to employ just one set of parameters for predicting life under different conditions and directions. To that intent, by adapting supplementary data, i.e., hysteresis loops, energy as a damage parameter will be employed and verified hereinafter.

3.2. Energy-Based Model

As demonstrated in Figure 5 and Figure 8, under stress-controlled condition the strain responses of the material are different along RD and ED. In addition, it has been presented in previous studies that the stress response of ZK60 extrusion under strain-controlled condition is dissimilar in these two directions [20]. Therefore, stress- and strain-based fatigue models may not explain the damage and fatigue life in different directions. On the other hand, strain energy is a quantity that incorporates both the stress and strain states of the material. Therefore, fatigue models which use strain energy as the damage parameter, are expected to provide an acceptable correlation between the damages in different material directions. Moreover, the scalar nature of strain energy enables this parameter to effectively account for the fatigue damage of the material under different loading conditions. Several studies have found the strain energy a promising candidate for describing the fatigue life of wrought Mg alloys exhibiting asymmetric and anisotropic characteristics [5], [12], [43], [62]. Jahed and Varvani [41] defined an energy-based damage parameter, similar to that in Ellyin's total strain energy model [31]:

$$\Delta E = \Delta E_e^+ + \Delta E_p \quad \text{Eq. 2}$$

where ΔE_e^+ and ΔE_p are elastic and plastic strain energy densities, respectively, and ΔE is total strain energy density and is considered as the JV damage parameter. ΔE_p is essentially the area inside the hysteresis loop, and $\Delta E_e^+$is calculated from $\sigma_{max}^2/2E$, in which E and σ_{max} are the Young's modulus and maximum stress, respectively. Figure 14 schematically illustrates the JV damage parameter's components. The elastic and plastic energy values are extracted from the half-life hysteresis loops.

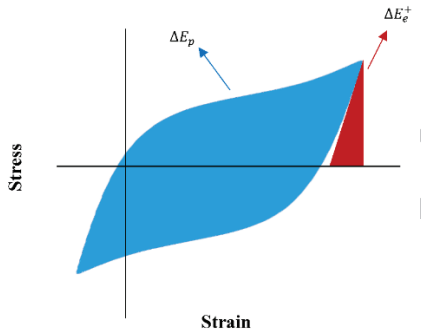

Figure 14. Illustration of elastic and plastic strain energy densities for JV model

The life correlation of the JV model is defined as follows:

$$\Delta E = E_e'(2N_f)^B + E_f'(2N_f)^C \quad \text{Eq. 3}$$

E_e', E_f', B, and C are energy-based material parameters. The coefficients E_e' and B are acquired by fitting a power curve into the experimental ESED, ΔE_e^+, and the coefficients E_f' and C are found from the experimental PSED, ΔE_p. The energy values for the stress-controlled tests were calculated using the half-life stress-strain response of the material in the two directions, Figure 5 (b) and Figure 8 (b). By utilizing TSED, ΔE, as the damage parameter, four sets of data including two sets from the current study and two from a previous strain-controlled study on the same material are plotted in Figure 15. As expected, it can be seen that all the data points, which were obtained from different loading conditions (stress- and strain-controlled) and loading directions (RD and ED), are consolidated into one curve. This observation agrees with previous works, which use strain energy as the damage parameter [63], [64]. Comparing Figure 13 and Figure 15 highlights the capability of energy-based models to predict the fatigue life of the material along different directions using a single set of material parameters. The physical basis of the energy-based

models is that the fatigue life is controlled by the strain energy that the material absorbs in each cycle. The soundness of energy approach in Mg alloys has been discussed in several studies [7], [16], [32], [34], [40].

The other observation from Figure 15 is that by utilizing the TSED to calculate the damage, the four different load cases were confined within a life band of x2. It suggests that irrespective of the ZK60 deformation mechanisms (slip in RD and twinning+slip in ED [20]), the corresponding TSED in a cycle governs the fatigue failure. Similar evidence was reported earlier for Mg alloys where energy associated with different loading phases in multiaxial loading were compared with one another and with uniaxial tension and cyclic shear [65], [66]. This observation implies that slip and twinning deformations are equally damaging and contributing to fatigue failure. However, verification of this hypothesis requires further investigation that is out of the scope of the present research.

Given that TSED consolidates the fatigue data regardless of the loading directions and conditions, it can predict the life of the material with a single set of parameters. The JV parameters in this study were extracted using all the data points included in Figure 15, and the fatigue life of the material along both RD and ED was predicted.

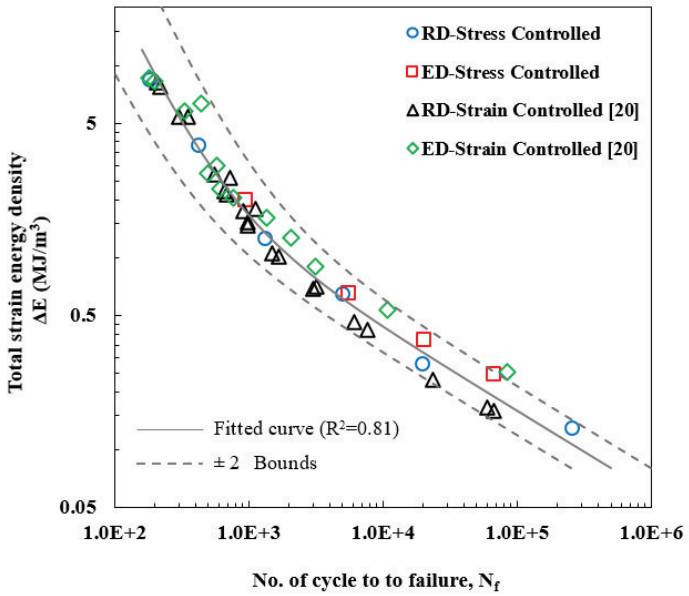

Figure 15. Energy-life curve for different loading conditions

Figure 16 (a) presents the life predicted by the JV model with respect to the experimental life. All the data points congregate tightly about the ideal estimation. The life prediction was excellent in the LCF, where the plastic deformation is significant and the PSED is the dominant term in the damage calculation (Eq. 2). However, in the HCF regime, where the PSED diminishes and the ESED takes over the fatigue damage, the life predictions slightly deviate from the experimental life.

In order to evaluate the prediction accuracy, the mean squared errors (MSE) between the n experimental and predicted lives at logarithmic scale were calculated, as follows:

$$MSE = \frac{\sum_{i=1}^{n}\left[Log(N_{Experimented}) - Log(N_{Predicted})\right]^2}{n} \quad \text{Eq. 4}$$

The MSE for stress-controlled tests in ED and RD is displayed and compared in Figure 16 (b). As shown in this figure, JV predicts the life with a good level of precision, irrespective of the loading direction.

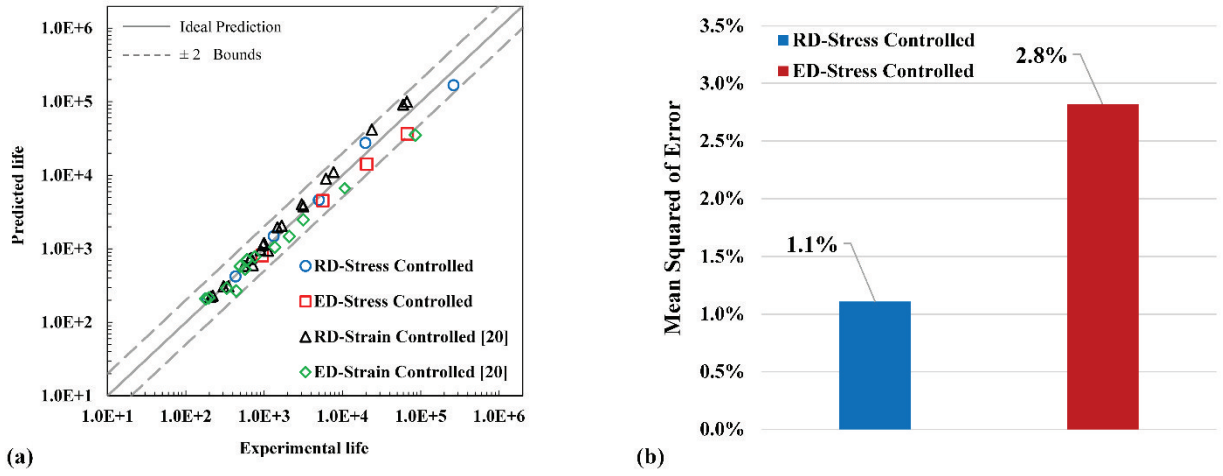

Figure 16. a) Predicted life vs. experimental life for both directions using one set of JV coefficients and b) Mean squared error for stress-controlled tests calculated for JV model

4. Conclusion

In this work, the stress-controlled fatigue behavior of ZK60 extrusion under uniaxial fully reversed loading was investigated and modeled along the material's extrusion (ED) and radial (RD) directions. The following conclusions summarize the findings:

1. Sigmoidal hysteresis loops with preserved symmetry were observed along RD under high-stress amplitudes because the twinning/detwinning deformations are active in both tension and compression reversals.
2. Loading along ED yields to asymmetric hysteresis response accompanied by considerable cyclic hardening when stress is adequately high to activate twinning/detwinning deformation.
3. The material along ED exhibits fatigue performance superior to that along RD in a wide range of stress amplitudes, due to ED's higher strength and consequently the smaller hysteresis loops.
4. The energy-based model can successfully correlate the fatigue life under stress-control condition in both directions.

References

[1] H. Friedrich and S. Schumann, "Research for a 'new age of magnesium' in the automotive industry," *J. Mater. Process. Technol.*, vol. 117, no. 3, pp. 276–281, 2001.

[2] M. M. Avedesian and H. Baker, *ASM specialty handbook: magnesium and magnesium alloys*. 1999.

[3] L. Wu *et al.*, "Twinning-detwinning behavior during the strain-controlled low-cycle fatigue testing of a wrought magnesium alloy, ZK60A," *Acta Mater.*, vol. 56, no. 4, pp. 688–695, 2008.

[4] J. Casey and H. Jahedmotlagh, "The strength-differential effect in plasticity," *Int. J. Solids Struct.*, vol. 20, no. 4, pp. 377–393, 1984.

[5] A. A. Roostaei and H. Jahed, "Role of loading direction on cyclic behaviour characteristics of AM30 extrusion and its fatigue damage modelling," *Mater. Sci. Eng. A*, vol. 670, pp. 26–40, 2016.

[6] J. B. Jordon *et al.*, "Investigation of fatigue anisotropy in an extruded magnesium alloy," *Int. J. Fatigue*, vol. 51, pp. 8–14, 2013.

[7] J. Dallmeier, O. Huber, H. Saage, and K. Eigenfeld, "Uniaxial cyclic deformation and fatigue behavior of AM50 magnesium alloy sheet metals under symmetric and asymmetric loadings," *Mater. Des.*, vol. 70, pp. 10–30, 2015.

[8] S.-H. Kim *et al.*, "Anisotropic in-plane fatigue behavior of rolled magnesium alloy with {10–12} twins," *Mater. Sci. Eng. A*, vol. 700, no. March, pp. 191–197, 2017.

[9] F. Lv *et al.*, "Tensile and low-cycle fatigue properties of Mg-2.8% Al-1.1% Zn-0.4% Mn alloy along the transverse and rolling directions," *Scr. Mater.*, vol. 61, no. 9, pp. 887–890, 2009.

[10] S. Ishihara, S. Taneguchi, H. Shibata, T. Goshima, and a. Saiki, "Anisotropy of the fatigue behavior of extruded and rolled magnesium alloys," *Int. J. Fatigue*, vol. 50, pp. 94–100, 2013.

[11] S. H. Park, S. G. Hong, W. Bang, and C. S. Lee, "Effect of anisotropy on the low-cycle fatigue behavior of rolled AZ31 magnesium alloy," *Mater. Sci. Eng. A*, vol. 527, no. 3, pp. 417–423, 2010.

[12] S. H. Park, S. G. Hong, J. Yoon, and C. S. Lee, "Influence of loading direction on the anisotropic fatigue properties of rolled magnesium alloy," *Int. J. Fatigue*, vol. 87, pp. 210–215, 2016.

[13] B. Marzbanrad, E. Toyserkani, and H. Jahed, "Cyclic hysteresis of AZ31B extrusion under load-control tests using embedded sensor technology," *Fatigue Fract. Eng. Mater. Struct.*, vol. 40, no. 2, pp. 221–232, Feb. 2017.

[14] S. Kleiner and P. J. Uggowitzer, "Mechanical anisotropy of extruded Mg-6% Al-1% Zn alloy," *Mater. Sci. Eng. A*, vol. 379, no. 1–2, pp. 258–263, 2004.

[15] Y. Xiong and Y. Jiang, "Cyclic deformation and fatigue of rolled AZ80 magnesium alloy along different material orientations," *Mater. Sci. Eng. A*, vol. 677, pp. 58–67, 2016.

[16] Y. C. Lin, X. M. Chen, Z. H. Liu, and J. Chen, "Investigation of uniaxial low-cycle fatigue failure behavior of hot-rolled AZ91 magnesium alloy," *Int. J. Fatigue*, vol. 48, no. C, pp. 122–132, 2013.

[17] C. Wang, T. J. Luo, J. X. Zhou, and Y. S. Yang, "Anisotropic cyclic deformation behavior of extruded ZA81M magnesium alloy," *Int. J. Fatigue*, vol. 96, pp. 178–184, 2017.

[18] Y. Xiong, X. Gong, and Y. Jiang, "Effect of initial texture on fatigue properties of extruded ZK60 magnesium alloy," *Fatigue Fract. Eng. Mater. Struct.*, vol. 274–276, no. I, pp. 193–198, Feb. 2018.

[19] L. Wu, "Mechanical Behavior and the Role of Deformation Twinning in Wrought Magnesium Alloys Investigated Using Neutron and Synchrotron X-ray Diffraction," 2009.

[20] A. H. Pahlevanpour, S. M. H. Karparvarfard, S. K. Shaha, S. B. Behravesh, S. Adibnazari, and H. Jahed, "Anisotropy in the quasi-static and cyclic behavior of ZK60 extrusion: Characterization and fatigue modeling," *Mater. Des.*, vol. 160, pp. 936–948, Dec. 2018.

[21] S. H. Park, "Effect of initial twins on the stress-controlled fatigue behavior of rolled magnesium alloy," *Mater. Sci. Eng. A*, vol. 680, no. September 2016, pp. 214–220, 2017.

[22] H. Gao, W. Ye, Z. Zhang, and L. Gao, "Ratcheting behavior of ZEK100 magnesium alloy with various loading conditions and different immersing time," *J. Mater. Res.*, vol. 32, no. 11, pp. 2143–2152, 2017.

[23] H. Zhang, D. X. Dong, S. J. Ma, C. F. Gu, S. Chen, and X. P. Zhang, "Effects of percent reduction and specimen orientation on the ratcheting behavior of hot-rolled AZ31B magnesium alloy," *Mater. Sci. Eng. A*, vol. 575, pp. 223–230, 2013.

[24] F. Lv *et al.*, "Fatigue properties of rolled magnesium alloy (AZ31) sheet: Influence of specimen orientation," *Int. J. Fatigue*, vol. 33, no. 5, pp. 672–682, 2011.

[25] O. H. Basquin, "The exponential law of endurance tests," *Proc. Am. Soc. Test. Mater.*, vol. 10, pp. 625–630, 1910.

[26] S. S. Manson, "Behavior of materials under conditions of thermal stress," *NACA Rep. TN 2933*, 1954.

[27] C. E. Feltner and J. D. Morrow, "Microplastic Strain Hysteresis Energy as a Criterion for Fatigue

Fracture," *J. Basic Eng.*, vol. 83, no. 1, p. 15, 1961.

[28] Y. S. Garud, "A New Approach to the Evaluation of Fatigue Under Multiaxial Loadings," *J. Eng. Mater. Technol.*, vol. 103, no. 2, p. 118, 1981.

[29] D. Lefebvre, K. W. Neale, and F. Ellyin, "A Criterion for Low-Cycle Fatigue Failure Under Biaxial States of Stress," *J. Eng. Mater. Technol.*, vol. 103, no. 1, p. 1, 1981.

[30] F. Ellyin and K. Golos, "Multiaxial Fatigue Damage Criterion," *J. Eng. Mater. Technol.*, vol. 110, no. 1, p. 63, 1988.

[31] F. Ellyin and D. Kujawski, "An energy-based fatigue failure criterion," *Microstruct. Mech. Behav. Mater.*, 1985.

[32] K. Shiozawa, J. Kitajima, T. Kaminashi, T. Murai, and T. Takahashi, "Low-cycle fatigue deformation behavior and evaluation of fatigue life on extruded magnesium alloys," *Procedia Eng.*, vol. 10, pp. 1244–1249, 2011.

[33] J. Dallmeier, O. Huber, H. Saage, K. Eigenfeld, and A. Hilbig, "Quasi-static and fatigue behavior of extruded ME21 and twin roll cast AZ31 magnesium sheet metals," *Mater. Sci. Eng. A*, vol. 590, pp. 44–53, 2014.

[34] S. Hyuk Park, S. G. Hong, B. Ho Lee, W. Bang, and C. Soo Lee, "Low-cycle fatigue characteristics of rolled Mg-3Al-1Zn alloy," *Int. J. Fatigue*, vol. 32, no. 11, pp. 1835–1842, 2010.

[35] S. Hasegawa, Y. Tsuchida, H. Yano, and M. Matsui, "Evaluation of low cycle fatigue life in AZ31 magnesium alloy," *Int. J. Fatigue*, vol. 29, no. 9–11, pp. 1839–1845, 2007.

[36] S. Ishihara, A. J. McEvily, M. Sato, K. Taniguchi, and T. Goshima, "The effect of load ratio on fatigue life and crack propagation behavior of an extruded magnesium alloy," *Int. J. Fatigue*, vol. 31, no. 11–12, pp. 1788–1794, 2009.

[37] J. O. Smith, "The Effect of Range of Stress on the Fatigue Strength of Metals," *Univ. Illinois, Eng. Exp. Station. Urbana,* vol. 334, pp. 631–636, 1942.

[38] K. N. Smith, T. H. Topper, and P. Watson, "A Stress-Strain Function for the Fatigue of Metals(Stress-Strain Function for Metal Fatigue Including Mean Stress Effect)," *J. Mater.*, vol. 5, pp. 767–778, 1970.

[39] S. K. Paul, S. Sivaprasad, S. Dhar, and S. Tarafder, "Ratcheting and low cycle fatigue behavior of SA333 steel and their life prediction," *J. Nucl. Mater.*, vol. 401, no. 1–3, pp. 17–24, 2010.

[40] G. Chen, L. T. Lu, Y. Cui, R. S. Xing, H. Gao, and X. Chen, "Ratcheting and low-cycle fatigue characterizations of extruded AZ31B Mg alloy with and without corrosive environment," *Int. J.*

Fatigue, vol. 80, no. August 2017, pp. 364–371, 2015.

[41] H. Jahed and A. Varvani-Farahani, "Upper and lower fatigue life limits model using energy-based fatigue properties," *Int. J. Fatigue*, vol. 28, no. 5–6, pp. 467–473, 2006.

[42] H. Jahed, A. Varvani-Farahani, M. Noban, and I. Khalaji, "An energy-based fatigue life assessment model for various metallic materials under proportional and non-proportional loading conditions," *Int. J. Fatigue*, vol. 29, no. 4, pp. 647–655, 2007.

[43] D. Toscano, S. K. Shaha, B. Behravesh, H. Jahed, and B. Williams, "Effect of forging on the low cycle fatigue behavior of cast AZ31B alloy," *Mater. Sci. Eng. A*, vol. 706, no. August, pp. 342–356, 2017.

[44] A. Gryguc *et al.*, "Monotonic and cyclic behaviour of cast and cast-forged AZ80 Mg," *Int. J. Fatigue*, vol. 104, pp. 136–149, 2017.

[45] S. M. H. Karparvarfard, S. K. Shaha, S. B. Behravesh, H. Jahed, and B. W. Williams, "Fatigue characteristics and modeling of cast and cast-forged ZK60 magnesium alloy," *Int. J. Fatigue*, no. November 2017, pp. 1–15, 2018.

[46] Y. Xiong, Q. Yu, and Y. Jiang, "Deformation of extruded ZK60 magnesium alloy under uniaxial loading in different material orientations," *Mater. Sci. Eng. A*, vol. 710, no. July 2017, pp. 206–213, 2018.

[47] H. Qiao, S. R. Agnew, and P. D. Wu, "Modeling twinning and detwinning behavior of Mg alloy ZK60A during monotonic and cyclic loading," *Int. J. Plast.*, vol. 65, pp. 61–84, 2015.

[48] R. R. I. R. R. I. R. R. I. Stephens *et al.*, "Metal fatigue in engineering," p. 496, 2001.

[49] M. Noban and H. Jahed, "Ratchetting strain prediction," *Int. J. Press. Vessel. Pip.*, vol. 84, no. 4, pp. 223–233, 2007.

[50] J. Albinmousa, H. Jahed, and S. Lambert, "Cyclic behaviour of wrought magnesium alloy under multiaxial load," *Int. J. Fatigue*, vol. 33, no. 8, pp. 1127–1139, 2011.

[51] Y. Xiong, Q. Yu, and Y. Jiang, "An experimental study of cyclic plastic deformation of extruded ZK60 magnesium alloy under uniaxial loading at room temperature," *Int. J. Plast.*, vol. 53, pp. 107–124, 2014.

[52] S. R. Agnew and Ö. Duygulu, "Plastic anisotropy and the role of non-basal slip in magnesium alloy AZ31B," *Int. J. Plast.*, vol. 21, no. 6, pp. 1161–1193, 2005.

[53] Z. Y. Nan, S. Ishihara, A. J. McEvily, H. Shibata, and K. Komano, "On the sharp bend of the S-N curve and the crack propagation behavior of extruded magnesium alloy," *Scr. Mater.*, vol. 56, no.

8, pp. 649–652, 2007.

[54] International Organization for Standardization, *ISO 12107-Metallic materials — Fatigue testing — Statistical planning and analysis of data*. 2003.

[55] S. P. Zhu, Q. Lei, and Q. Y. Wang, "Mean stress and ratcheting corrections in fatigue life prediction of metals," *Fatigue Fract. Eng. Mater. Struct.*, vol. 40, no. 9, pp. 1343–1354, 2017.

[56] S.-P. Zhu, Q. Lei, H.-Z. Huang, Y.-J. Yang, and W. Peng, "Mean stress effect correction in strain energy-based fatigue life prediction of metals," *Int. J. Damage Mech.*, vol. 26, no. 8, pp. 1219–1241, 2016.

[57] S. J. Park, K. S. Kim, and H. S. Kim, "Ratcheting behaviour and mean stress considerations in uniaxial low-cycle fatigue of Inconel 718 at 649 °C," *Fatigue Fract. Eng. Mater. Struct.*, vol. 30, no. 11, pp. 1076–1083, 2007.

[58] S. Begum, D. L. Chen, S. Xu, and A. A. Luo, "Effect of strain ratio and strain rate on low cycle fatigue behavior of AZ31 wrought magnesium alloy," *Mater. Sci. Eng. A*, vol. 517, no. 1–2, pp. 334–343, 2009.

[59] S. Begum, D. L. Chen, S. Xu, and A. A. Luo, "Strain-controlled low-cycle fatigue properties of a newly developed extruded magnesium alloy," *Metall. Mater. Trans. A Phys. Metall. Mater. Sci.*, vol. 39, no. 12, pp. 3014–3026, 2008.

[60] G. Kang, C. Yu, Y. Liu, and G. Quan, "Uniaxial ratchetting of extruded AZ31 magnesium alloy: Effect of mean stress," *Mater. Sci. Eng. A*, vol. 607, no. June, pp. 318–327, 2014.

[61] B. Marzbanrad, E. Toyserkani, and H. Jahed, "Cyclic hysteresis of AZ31B extrusion under load-control tests using embedded sensor technology," *Fatigue Fract. Eng. Mater. Struct.*, vol. 40, no. 2, pp. 221–232, 2017.

[62] F. Castro and Y. Jiang, "Fatigue life and early cracking predictions of extruded AZ31B magnesium alloy using critical plane approaches," *Int. J. Fatigue*, vol. 88, pp. 236–246, 2016.

[63] H. Jahed and J. Albinmousa, "Multiaxial behaviour of wrought magnesium alloys - A review and suitability of energy-based fatigue life model," *Theor. Appl. Fract. Mech.*, vol. 73, pp. 97–108, 2014.

[64] Y. Ling, A. A. Roostaei, G. Glinka, and H. Jahed, "Fatigue of ZEK100-F magnesium alloy: Characterisation and modelling," *Int. J. Fatigue*, vol. 125, pp. 179–186, 2019.

[65] J. Albinmousa, H. Jahed, and S. Lambert, "Cyclic axial and cyclic torsional behaviour of extruded AZ31B magnesium alloy," *Int. J. Fatigue*, vol. 33, no. 11, pp. 1403–1416, 2011.

[66] A. A. Roostaei and H. Jahed, "Multiaxial cyclic behaviour and fatigue modelling of AM30 Mg alloy extrusion," *Int. J. Fatigue*, vol. 97, pp. 150–161, 2017.

- Sigmoidal but symmetric hysteresis loops are observed in radial direction.
- First reversal being tensile or compressive does not affect strain amplitude and life.
- Ratchetting direction in radial and extrusion directions are opposite.
- The extrusion direction exhibits superior stress-controlled fatigue performance.
- Energy-based fatigue parameters correlate life in radial and extrusion directions.